



7th International Conference on Fatigue Design, Fatigue Design 2017,
29-30 November 2017, Senlis, France

Optimization of fretting resistance of modular stem

Philippe Amuzuga^{1,*}, Yanneck Suchier¹ and Fabien Lefebvre¹

¹Centre technique des industries mécaniques,
7, rue de la Presse, CS 50802, 42952 Saint-Etienne Cedex 1, France.

Abstract

The modular neck hip prostheses mechanical failure can have several causes, separated or combined such as fretting, corrosion, wear and fatigue. Corrosion mechanism is overcome by specific heat treatment. The fatigue mechanism occurrence is delayed by forging process coupled with finishing process such as shot peening. The breakage of the modular neck becomes mainly related to fretting issues. This is firstly due to the amplitudes of micro-movements of a mismatched geometric tolerance. The effect of contact condition on the fretting behaviour should also be put in relationship with to the used material performances. This study aims to highlight the effect of design parameters on the modular stem fretting resistance. The overall analysis of the results from the design of experiments carried out have shown that a trade-off should to be found between parameters since their variation could be beneficial for fretting wear resistance while becoming unfavorable for fretting fatigue, according to the evaluation criteria.

© 2018 The Authors. Published by Elsevier Ltd.

Peer-review under responsibility of the scientific committee of the 7th International Conference on Fatigue Design.

Keywords:

* Corresponding author. Tel.: +33 477 794148;
E-mail address: philippe.amuzuga@cetim.fr

1. INTRODUCTION

It has been observed that the assembly method [1] (by hand or by impact[†]) as well as the force magnitude [2], direction [3] and location [4], used to compact a modular implant could influence its fretting behavior. Viceconti [5], [6] highlights the influence of the design on the stem/neck junction fretting behavior. It has been shown that a thinner stem diameter reduce the wear by following the neck displacement through elastic deformation. This limits relative micro-displacements then decreases fretting. In addition, an oblong section has been identified as the optimal geometry that minimized the mechanical stress for the same material volume. Otherwise, the stem diameter reduction leads to limit micro-motion. Surface roughness can be used to control the stick and slip zone within the effective contact area. Kretzer's work [7] shows that increase surface roughness tends to decrease the salted-out particles quantity. However care must be taken not to produce a notch effect that occurs when roughness is not adequately controlled. This will increase the risk of surface cracking and generate some relatively large size debris. However roughness increases the contact pressure then augments the stress level underneath. When the maximum principal stress is located close to the outermost surface layer, this leads to crack nucleation and propagation over cycles. This failure mode falls within the scope of contact fatigue framework. A presence of an initial residual compressive stress left by thermo-chemical treatments and shot peening process, prevent the surface layer from this fatigue phenomena.

Moreover, it has been reported in [8] that with small micro motions or high normal pressures, low fretting damage was observed. Increase the effective contact area enables a greater proportion of a stick zone than the slip zone then finally decrease micro-motions. But fretting phenomena is complex and cannot be controlled only by the normal pressure. By determining critical location for crack initiation and crack inclination based on Dang Van criterion, M.C. Baietto et al.[9] have shown how the crack length, the tangential loading modify the crack path during the propagation process over fretting cycles.

All things gathered, three majors fretting mechanisms [10], [11] have been identified: (i) fretting wear concerning the abrasion or seizure with production of wear particles; (ii) fretting fatigue standing for the phenomenon of prevalent adhesion initiating surface micro-cracks; (iii) fretting corrosion mixing the effect of environment conditions [12] (oxygen concentration, local pH, body temperature), material microstructure (phases, grain boundaries) and cinematic (high velocity increase mass transfer rate). There are some interaction and competition between these different fretting mechanisms. It should be kept in mind that, in all case, the intensification of one of these fretting mechanisms always worsens the others. For a typical scenario: fretting fatigue → micro-cracks → oxygen migration from the ambient liquid to an entrapment inside growing crack cavities → fretting corrosion → hard oxide particles releasing → abrasion of the contacting surfaces → fretting wear. Moreover the degradation phenomena could be accelerated or slowed owing to the formed third body characteristic this is well known to drastically influence the contact conditions [13]. Furthermore, titanium and cobalt chromium alloys are the main materials used for the modular stem. Using same alloy for the stem and the neck often led to the seizure then complicates the extraction of the modular neck from the stem. Additionally that could lead to inter granular corrosion. But using different materials can also lead to galvanization corrosion. It should be specified that the corrosion decrease surface property and topology. This leads to accelerate fretting phenomena [14] and fatigue failure because the neck section reduction increase stress range. Note that corrosion phenomena are mostly observed for cobalt chromium alloys [15]. The implants surface engineering processes have been found to influence the fretting wear behavior. The fretting wear test device developed in [16] to reproduce in vivo motion at the titanium implants interfaces, have been carried out that after 1.5 million cycles, the test using bone against a rougher plasma-sprayed surface has produced greater wear

[†] An impact assembly method mimics a hammer blows force applications.

compared to that of a fiber-mesh surface. Recent study [17] considers design parameters and the friction behavior as decisive for fretting wear severity. The neck/shaft angle is found to be an effective tool to reduce fretting corrosion issues. Statistical analysis conducted in [18] revealed that a more obtuse neck/shaft angle tends to enhance the implant resistance to failure. Hence the present work aims to investigate the fretting resistance of modular stem according to design and material parameters. Comparative analysis has been conducted based on results from three set of design of experiments.

2. METHODS

Finite element analysis has been performed using ANSYS Workbench. The geometry of assembled parts has been simplified as presented in Fig. 2. Materials are considered isotropic, elastic and homogeneous. Linear quasi-static analysis has been conducted. Plastic and thermic strain fields resulting from manufacturing and finishing process are not included. This implied that residual stresses coming from these permanent strains are not taking into account. It is worth specifying that these residual stresses are generally benefit for components since they prevent from further plastic yielding. Note that the finite element analysis is conducted under small strain assumptions.

Units used during this study are:

- Mega Pascal (MPa) for mechanical stresses and pressure
- Newton (N) for forces
- Micro meter (μm) for lengths
- Degree ($^\circ$) for angles

The nomenclature used during this study is:

SWT Smith-Watson-Tooper
 DoE Design of experiment
 μ Coefficient of friction
 E Young's modulus
 ν Poisson ratio
 F Assembly force
 L Neck length
 H Neck height
 A Neck angle
 t Upper face tolerance on the neck angle
 t_{lat} Lateral face tolerance on the neck angle
 δ_{Max} Total sliding distance
 P_{max} Maximum contact pressure
 σ_{max} Maximum principal stress
 τ_{max} Maximum shear stress

2.1 Model

The model relies mainly on the use of volume elements. The mesh characteristics will not be presented here.

2.1.1 Geometry and materials

Fig.1 illustrates the modular hip prosthesis.

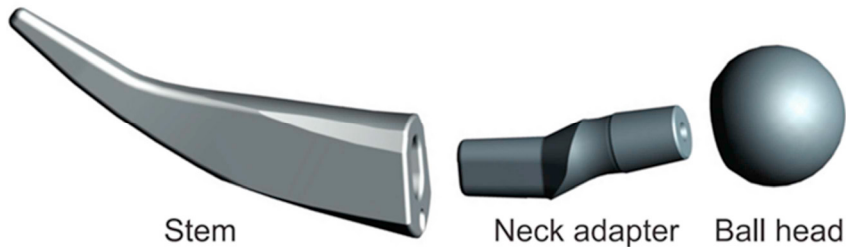


Figure1. Modular hip prosthesis [18]

Tab. 1 list the different materials used in this study along with their engineering data.

Component	Materials	E(GPa)	ν
Stem	TA6V	110	0.33
Neck	TA6V/CoCr	110/235	0.33

Table 1. Materials

2.1.2 Loading and Fixtures

The stem is constrained by assigning no displacement as shown in Fig. 2. Two loadings have been applied as illustrated in Fig. 3. The first cycle represents the assembly force and the others stand for the functional force. Every cycle is composed by a loading time step followed by an unloading.

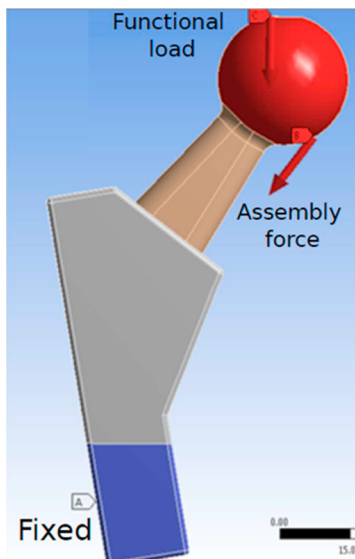


Figure2. Load and fixture definition

Colloque Supméca 2017

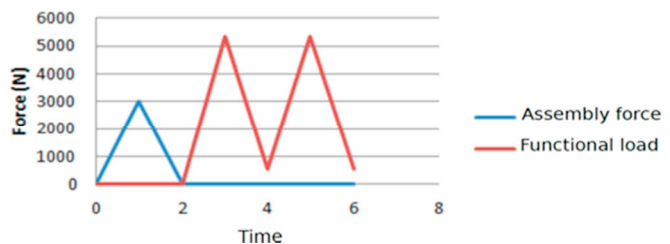


Figure3. Loading path

2.1.3 Parametric study

Fig. 4 schematizes the modular prosthesis neck design parameters. It should be specified that the input parameter values presented in Tab. 2, have been chosen in accordance with the values encountered in practice.

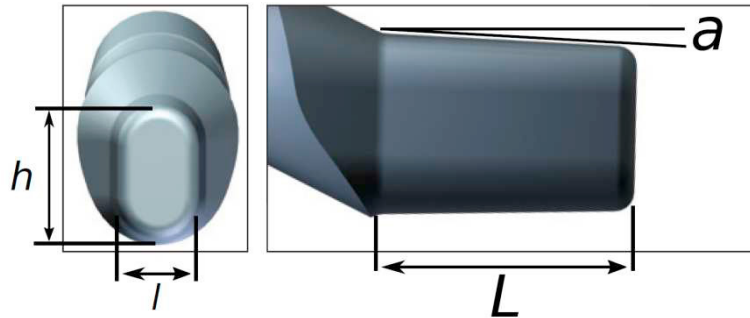


Figure4. Neck design parameters [18]

Table2. DoE parameters

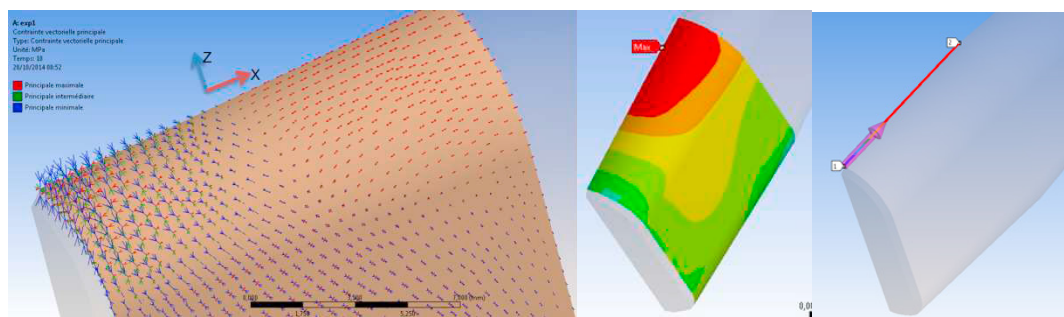
Parameters	Min value	Max value
μ	0.1	0.8
E (GPa)	110	235
F (MPa)	300	6 000
L (mm)	15	17
H (mm)	17	19
α (°)	2	3
t (°)	-0.1	0.1
t _{lat} (°)	-0.1	0.1

2.2 Evaluation criteria

The fretting fatigue and fretting wear evaluation are both based on energy criteria. Let’s specify that the wear criteria are calculated via APDL script on ANSYS Workbench while the fatigue criteria are post-treated on Matlab.

2.2.1 Fretting fatigue criterion

Smith-Watson-Tooper (SWT) fatigue criterion is used in this study to evaluate the fretting fatigue severity for the DoE different configurations. The SWT is expressed by Eq. (4) (see Appendix). Tomography diagnostic conducted in [15] revealed no material defects or stress risers inside similar implant material used in the present study. It means that failure is essentially due to materials interface conditions. Hence there is no need to compute criteria inside the volume. Also, for simplification purpose the SWT criteria have been computed on the neck surface following the line indicated in Fig. 5(c). The critical zone has been identified to be located at the upper surface of the neck recessed as shown in Fig. 5(b). This is consistent with fatigue crack initiation zone observed experimentally. On this upper surface, compressive stress is generated perpendicular to the neck length direction leading to a tensile stress over the X-axis as in Fig. 5(a). Knowing that crack will be initiated along the principal tensile stress direction, the critical plane of the SWT criterion is thus sought in the plane (X, Z) plotted in Fig. 5.



(a) Principal stress vectors (b) Tensile principal stress (c) SWT evaluation line
Figure 5. SWT computation on the neck surface

2.2.3 Fretting wear criterion

Archard [19] wear criterion is used in this study to evaluate the fretting wear severity for the DoE different configurations. The wear volume is expressed by Eq. (3) (see Appendix). Lately, Popov et al.[20] have developed fretting wear calculation model which has reduced drastically simulation time but their procedure is limited to rotationally symmetric contact profile.

3. RESULTS AND DISCUSSION

The DoE are performed by following a Taguchi's orthogonal array [21]. The obtained results are listed in Tab. 3, Tab. 5 and Tab. 7. Displacement, pressure and stress fields are used to calculate the aforementioned evaluation criteria. Let's recall that this study presents comparative analysis based on criteria value obtained from different configurations. Predictive analysis could be conducted by integrating micro plasticity coupled with damage and wear models [22], [23], [24].

3.1 Global influence of DoE parameters

The first DoE presented in Tab. 3 aim to analyze the influence of all the parameters considered in the study. An overview of the results from the first DoE indicated a smaller scattering on the SWT criteria than that of the wear. It could be noticed that the assembly force has a significant impact on the fretting fatigue. The other parameters produced a small dispersion on the SWT for $F = 3150\text{N}$. The dispersion increased for $F = 6000\text{N}$. It could be argued that very high assembly force generated large deformation then exhibits the SWT sensitivity to the other parameters. High values of E , L and t seem to enhance the fretting fatigue resistance. But a gives it best results for low value. However H and t analysis not allows highlighting significant trends on the SWT. Furthermore μ , t and H act to decrease the wear. Concerning the materials, CoCr presents a better fretting fatigue resistance than TA6V. But their effect is reversed when regarding fretting wear resistance. All things considered, to minimize both criteria simultaneously, this study could recommend a tolerance in a range of $t = 0.1^\circ$ with an assembly force of about $F = 3150\text{N}$. These values should be interpreted as the configuration which trends

to privilege the stem/neck contact on the interface entrance more than deep.

Table3. Result from first DoE

Exp N°	E GPa	F N	H mm	L mm	a °	t °	t _{lat} °	μ -	δ ^{Max} μm	p ^{max} MPa	σ ^{max} MPa	τ ^{max} MPa	SWT -	Wear -
1	110	300	18	15	2	-0,1	-0,1	0,1	124	466	269	134	0.376	1469
2	110	300	18,5	16	2,5	0	0	0,45	24	80	298	141	0.372	71.3
3	110	300	19	17	3	0,1	0,1	0,8	28	96	316	164	0.440	61.3
4	110	3150	18	15	2,5	0	0,1	0,8	25	84	351	165	0.530	52.4
5	110	3150	18,5	16	3	0,1	-0,1	0,1	32	301	265	130	0.339	888
6	110	3150	19	17	2	-0,1	0	0,45	23	66	279	139	0.362	67.6
7	110	6000	18	16	2	0,1	0	0,8	28	145	520	291	1.389	122
8	110	6000	18,5	17	2,5	-0,1	0,1	0,1	61	542	585	252	1.443	2116.1
9	110	6000	19	15	3	0	-0,1	0,45	29	184	625	287	1.642	156.1
10	235	300	18	17	3	0	0	0,1	53	558	584	265	0.729	1737
11	235	300	18,5	15	2	0,1	0,1	0,45	25	223	575	267	0.664	137.9
12	235	300	19	16	2,5	-0,1	-0,1	0,8	16	96	640	308	0.822	97.9
13	235	3150	18	16	3	-0,1	0,1	0,45	21	104	355	159	0.244	72.9
14	235	3150	18,5	17	2	0	-0,1	0,8	18	78	266	140	0.144	65
15	235	3150	19	15	2,5	0,1	0	0,1	33	346	278	120	0.151	80.7
16	235	6000	18	17	2,5	0,1	-0,1	0,45	25	200	510	255	0.629	154.6
17	235	6000	18,5	15	3	-0,1	0	0,8	25	169	743	350	1.108	104.6
18	235	6000	19	16	2	0	0,1	0,1	56	590	5418	234	0.598	1866.1
								Mean	35,9	240,4	715,4	211,2	0,7	518

3.2 Effect of L, a and t_{lat}

The second DoE presented in Tab. 5 aim to analyze the influence of L, a and t_{lat} while the other parameters are set as in Tab. 4.

Table 4. Fixed parameter value for the second DoE

Parameter Value	E	F	μ	H	t
	110GPa	3150N	0.45	19mm	0.1°

It could be observed from Tab. 5 that, for the SWT criterion, this second DoE confirms the trends observed previously. To increase fretting fatigue resistance, the values of a and t_{lat} must be minimized while that of L must be maximized. It can also be noted that the interactions between parameters become negligible. Otherwise, about the wear criterion, the effects found during the first DoE for t_{lat} and L have been conserved. However there is a strong interaction between these two parameters for the fretting wear behavior. Two consequences arise from the interaction between t_{lat} and L:

- On one hand, it is beneficial for the fretting fatigue to increase L and decrease t_{lat}. However the augmentation of L reduces the influence of t_{lat}.
- On the other hand, it is harmful for the fretting wear to increase L unless one increases t_{lat} at the same time. Moreover, a modification of t_{lat} generates more change on the wear than on the fatigue.

One can conclude that a trade-off should be found between fretting fatigue and fretting wear resistance. This is consistent with statements found in the literature for most studies which evaluated the effect of design parameters on fretting.

Table5. Result from second DoE

Exp N°	L	a	t_{lat}	δ^{max}	p^{max}	σ^{max}	τ^{max}	SWT	Wear
	mm	$^\circ$	$^\circ$	μm	MPa	MPa	MPa	-	-
1	15	2	-0,1	21	61	260	122	0.273	64.1
2	15	2	0	23	72	273	126	0.315	65.3
3	15	2	0,1	24	84	277	127	0.312	56.6
4	16	2	-0,1	21	64	239	114	0.243	70.3
5	16	2	0	23	73	254	122	0.275	65.8
6	16	2	0,1	24	89	260	118	0.275	59.1
7	17	2	0	23	76	237	113	0.248	72.7
8	17	2	0,1	25	92	250	114	0.259	62.1
9	17	2	-0,1	19	69	216	108	0.243	77.9
10	15	3	0,1	26	91	289	133	0.340	63.5
11	15	3	-0,1	23	59	290	131	0.323	65.3
12	15	3	0	25	73	297	135	0.361	66.8
13	16	3	0	24	76	280	132	0.322	71.8
14	16	3	0,1	26	94	276	125	0.312	66
15	16	3	-0,1	21	64	255	118	0.258	72.4
16	17	3	0,1	26	98	262	120	0.287	68.7
17	17	3	-0,1	21	68	231	111	0.249	79.2
18	17	3	0	25	79	260	122	0.289	78.8
			Mean	23,3	76,8	261,4	121,7	0.3	68

3.3 Effect of the assembly force and friction coefficient

The third DoE set t_{lat} and L at their highest value (see Tab.6) in order to investigate F and μ influence on the fretting fatigue and fretting wear. The result is filled in Tab. 7.

Table 6. Fixed parameter value for the third DoE

Parameter	E	L	a	H	t	t_{lat}
Value	110GPa	17mm	2°	19mm	0.1°	0.1°

It could be seen from Fig.6 that $\mu = 0.4$ minimizes the friction coefficient unfavorable effect on fretting fatigue behaviour regardless of the applied assembly force. In addition, high assembly force seems to be less efficient for low friction coefficient but allows having a beneficial effect when the friction coefficient is getting higher. It could be seen in Fig. 7 that the friction coefficient decreases the wear criterion and leads to an asymptotic behavior from $\mu = 0.4$ whatever of the assembly force.

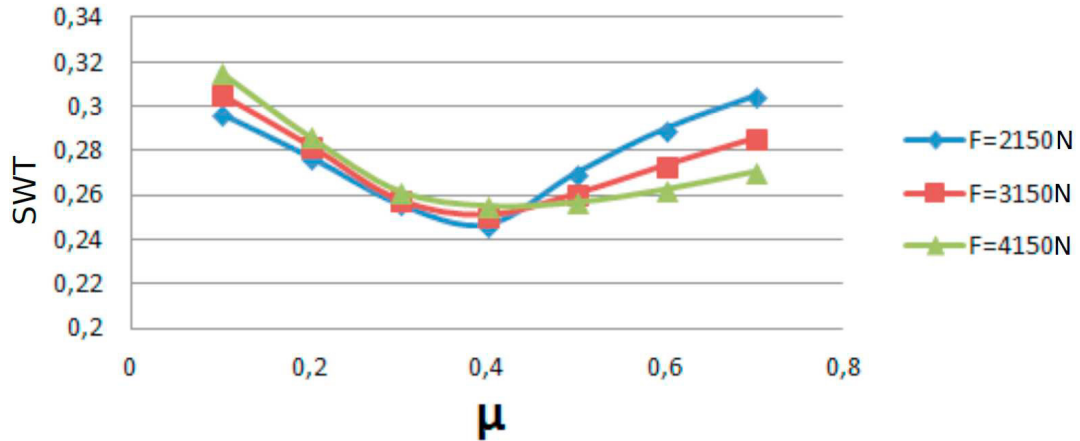
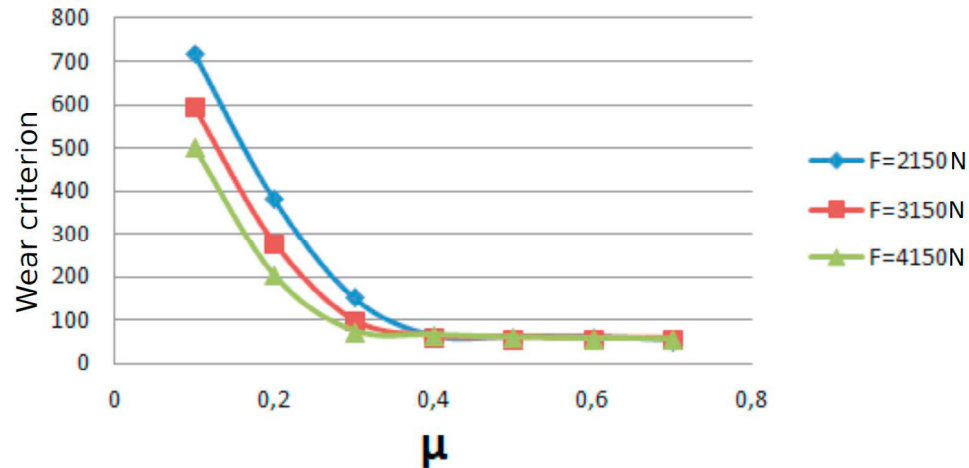


Figure6. Effect of F and μ according to SWT

However high assembly force reduces the fretting wear for low friction coefficients. Note that after passing the critical value of $\mu = 0.4$, neither the assembly force nor the friction coefficient significantly affects the wear criterion. By analyzing the effect of friction coefficient for values of 0.5, 0.75 and 1 Sadeghi et al. [25] noticed that the wear rate or the wear initiation period was not affected significantly. This supported the present study results. One can argue that for a given design parameters, there is a threshold value of the friction coefficient which could condition the passage between the slip, adherence and mixed regimes during the fretting contact. This could explain here the effect on the fretting behaviour for $\mu = 0.4$. Vingsbo and Soderberg [26] emphasized that in fretting contact, the partial slip regime is the most deleterious for fretting fatigue life and fretting wear rate variation with the displacement amplitude and with the applied normal force [27]. Also, cracking behavior analysis by using critical-plane SWT fatigue damage approach [28] revealed longer crack lengths within the slip zones.

Figure7. Effect of F and μ according to wear criterion

Exp N°	F	μ	δ^{max}	P^{max}	σ^{max}	τ^{max}	SWT	Wear
	N	-	μm	MPa	MPa	MPa	-	-
1	2150	0.1	58	314	269	111	0.297	599.2
2	2150	0.2	55	225	241	113	0.277	282.5
3	2150	0.3	44	151	246	111	0.256	101.2
4	2150	0.4	28	96	248	114	0.247	63.5
5	2150	0.5	26	93	257	117	0.270	60.7
6	2150	0.6	26	92	263	122	0.290	59.3
7	2150	0.7	25	90	265	123	0.305	58.3
8	3150	0.1	39	274	279	111	0.306	719.7
9	3150	0.2	40	190	246	113	0.283	382
10	3150	0.3	31	119	245	111	0.258	152.4
11	3150	0.4	25	94	248	112	0.251	63.5
12	3150	0.5	25	91	249	115	0.261	61.4
13	3150	0.6	25	91	253	121	0.274	60.3
14	3150	0.7	25	92	255	122	0.286	54.3
15	4150	0.1	28	235	289	110	0.315	503.9
16	4150	0.2	31	158	249	112	0.286	205.4
17	4150	0.3	25	99	247	110	0.262	75.9
18	4150	0.4	24	92	245	110	0.255	65.5
19	4150	0.5	22	89	243	111	0.257	60.2
20	4150	0.6	23	89	245	112	0.262	57.4
21	4150	0.7	24	90	247	11	0.270	56.6
		Mean	27.6	128.8	252.9	105.8	0.3	178

Table7. Result from third DoE

4. CONCLUSION

The simulation carried out on the modular stem allow to better understanding how some identified design parameters influence the contact conditions considerably (micro-displacement, contact pressure) then the fretting resistance. It can be noted that these conditions exhibit large dispersion as a function of the geometrical parameters (in particular the tolerances). The total slip distance has been raised between 20 and 100 μm while the contact pressures varied between 300 and 800MPa. The DoE have highlighted the most influential factors in the design parameters as the coefficient of friction the assembly force and the angular tolerances. This study shows the modular stem main improvement approaches, particularly the interface adaptation, in order to obtain the ideal coefficient of friction ($\mu = 0.4$ here) which minimizes the risk of fretting wear and fatigue. Otherwise, the necessity of biocompatibility is a constraint on the choice of materials. It has been found that the use of Titanium alloy augments the risk of the neck fracture more than cobalt chromium alloy. But the latter increases the production of wear particles that are potentially harmful to the patient body. Moreover the use of the couple TA6V/CrCo could be at the origin of galvanization corrosion. Let us note finally that the optimization of the contact conditions requires a numerical model which is able to determine the best configuration of the parameters set.

Acknowledgments

The authors would like to acknowledge LTDS, Ecole Centrale de Lyon and Mines Saint Etienne teams for their involvement and motivation in our joint projects. CETIM would like to acknowledge its partners HEF IREIS, Thermi-Lyon, SEEP and SEM for funding and permission to publish this work.

Appendix

The evaluation criteria used in the present study are expressed hereafter.

Wear criteria

The wear volume V is estimated as:

$$V = k \int_0^L \delta_{\max} \times FT - Ed_{th} \quad (1)$$

Where k is the Archard wear coefficient, L is the total sliding distance, Ed_{th} is the energy threshold for wear activation, FT is the tangential contact force. In full slip regime (1) becomes:

$$V = k \int_0^L \delta_{\max} \times \mu \times FN - Ed_{th} \quad (2)$$

Where μ is the coefficient of friction and FN is the normal contact force. FN is calculated with the contact pressure P_{\max} and the contact surface S . The wear criteria used in the present study is expressed as the volume over the wear coefficient offset by Ed_{th} :

$$\text{Wear} = V/k + Ed_{th} = \int_0^L \delta_{\max} \times \mu \times P_{\max} \times S \quad (3)$$

SMITH -WATSON -TOPPER criteria

The SWT criterion is expressed as:

$$\text{SWT} = \max (\epsilon_a \times \sigma_{\max}) \quad (4)$$

Where ϵ_a is the total strain amplitude and σ_{\max} maximum principal stress.

References

- [1] F. Aljenaei, I. Catelas, H. Louati, P. E. Beaulé, et M. Nganbe, « Effects of Hip Implant Modular Neck Material and Assembly Method on Fatigue Life and Distraction Force », *J. Orthop. Res.*, 2017.
- [2] K. A. Abdullah, *Stress and stability analysis of the neck-stem interface of the modular hip prosthesis*. Queen's University at Kingston, 1998.
- [3] T. Bitter, D. Janssen, B. W. Schreurs, T. Marriott, I. Khan, et N. Verdonschot, « THE EFFECT OF ASSEMBLY FORCE AND ANGLE ON CONTACT PRESSURES AND MICROMOTIONS AT THE TAPER JUNCTION OF MODULAR HIP IMPLANTS », *Bone Jt. J.*, vol. 98, n° SUPP 1, p. 48–48, 2016.
- [4] M. L. Mroczkowski, J. S. Hertzler, S. M. Humphrey, T. Johnson, et C. R. Blanchard, « Effect of impact assembly on the fretting corrosion of modular hip tapers », *J. Orthop. Res.*, vol. 24, n° 2, p. 271–279, 2006.
- [5] M. Viceconti, M. Baleani, S. Squarzone, et A. Tonil, « Fretting wear in a modular neck hip prosthesis », *J. Biomed. Mater. Res. A*, vol. 35, n° 2, p. 207–216, 1997.
- [6] M. Viceconti, O. Ruggeri, A. Toni, et A. Giunti, « Design-related fretting wear in modular neck hip prosthesis », *J. Biomed. Mater. Res. A*, vol. 30, n° 2, p. 181–186, 1996.
- [7] J. P. Kretzer, E. Jakubowitz, M. Krachler, M. Thomsen, et C. Heisel, « Metal release and corrosion effects of modular neck total hip arthroplasty », *Int. Orthop.*, vol. 33, n° 6, p. 1531, 2009.
- [8] M. Baxmann, S. Y. Jauch, C. Schilling, W. Blömer, T. M. Grupp, et M. M. Morlock, « The influence of contact conditions and micromotions on the fretting behavior of modular titanium alloy taper connections », *Med. Eng. Phys.*, vol. 35, n° 5, p. 676–683, 2013.
- [9] M.-C. Baietto, E. Pierres, et A. Gravouil, « A multi-model X-FEM strategy dedicated to frictional crack growth under cyclic fretting fatigue loadings », *Int. J. Solids Struct.*, vol. 47, n° 10, p. 1405–1423, 2010.
- [10] J. D. Boby, J. P. Collier, M. B. Mayor, T. McTighe, M. Tanzer, et B. K. Vaughn, « Particulate debris in total hip arthroplasty: Problems and solutions Scientific Exhibit », in *AAOS Annual Meeting*, 1993.
- [11] A. Srinivasan, E. Jung, et B. R. Levine, « Modularity of the femoral component in total hip arthroplasty », *J. Am. Acad. Orthop. Surg.*, vol. 20, n° 4, p. 214–222, 2012.
- [12] L. Duisabeau, P. Combrade, et B. Forest, « Environmental effect on fretting of metallic materials for orthopaedic implants », *Wear*, vol. 256, n° 7, p. 805–816, 2004.
- [13] S. Basseville, E. Héripéré, et G. Cailletaud, « Numerical simulation of the third body in fretting problems », *Wear*, vol. 270, n° 11, p. 876–887, 2011.
- [14] P. Wodecki, D. Sabbah, G. Kermarrec, et I. Semaan, « New type of hip arthroplasty failure related to modular femoral components: breakage at the neck-stem junction », *Orthop. Traumatol. Surg. Res.*, vol. 99, n° 6, p. 741–744, 2013.
- [15] P. Norman, S. Iyengar, I. Svensson, et G. Flivik, « Fatigue fracture in dual modular revision total hip arthroplasty stems: failure analysis and computed tomography diagnostics in two cases », *J. Arthroplasty*, vol. 29, n° 4, p. 850–855, 2014.
- [16] E. Ebramzadeh, F. Billi, S. N. Sangiorgio, S. Mattes, W. Schmoelz, et L. Dorr,

- « Simulation of fretting wear at orthopaedic implant interfaces », *J. Biomech. Eng.*, vol. 127, n° 3, p. 357–363, 2005.
- [17] S. Y. Jauch, G. Huber, H. Haschke, K. Sellenschloh, et M. M. Morlock, « Design parameters and the material coupling are decisive for the micromotion magnitude at the stem–neck interface of bi-modular hip implants », *Med. Eng. Phys.*, vol. 36, n° 3, p. 300–307, 2014.
- [18] H. Haschke, S. Y. Jauch-Matt, K. Sellenschloh, G. Huber, et M. M. Morlock, « Assembly force and taper angle difference influence the relative motion at the stem–neck interface of bi-modular hip prostheses », *Proc. Inst. Mech. Eng. [H]*, vol. 230, n° 7, p. 690–699, 2016.
- [19] J. F. Archard et W. Hirst, « The wear of metals under unlubricated conditions », in *Proceedings of the Royal Society of London A: Mathematical, Physical and Engineering Sciences*, 1956, vol. 236, p. 397–410.
- [20] A. V. Dimaki, A. I. Dmitriev, Y. S. Chai, et V. L. Popov, « Rapid simulation procedure for fretting wear on the basis of the method of dimensionality reduction », *Int. J. Solids Struct.*, vol. 51, n° 25, p. 4215–4220, 2014.
- [21] G. Taguchi et G. Taguchi, « System of experimental design; engineering methods to optimize quality and minimize costs », 1987.
- [22] F. Shen, W. Hu, et Q. Meng, « A damage mechanics approach to fretting fatigue life prediction with consideration of elastic–plastic damage model and wear », *Tribol. Int.*, vol. 82, p. 176–190, 2015.
- [23] T. Zhang, N. M. Harrison, P. F. McDonnell, P. E. McHugh, et S. B. Leen, « Micro–macro wear–fatigue of modular hip implant taper-lock coupling », *J. Strain Anal. Eng. Des.*, vol. 49, n° 1, p. 2–18, 2014.
- [24] A. M. Tobi, J. Ding, G. Bandak, S. B. Leen, et P. H. Shipway, « A study on the interaction between fretting wear and cyclic plasticity for Ti–6Al–4V », *Wear*, vol. 267, n° 1, p. 270–282, 2009.
- [25] A. Ghosh, B. Leonard, et F. Sadeghi, « A stress based damage mechanics model to simulate fretting wear of Hertzian line contact in partial slip », *Wear*, vol. 307, n° 1, p. 87–99, 2013.
- [26] O. Vingsbo et S. Söderberg, « On fretting maps », *Wear*, vol. 126, n° 2, p. 131–147, 1988.
- [27] E. J. Berger, « Friction modeling for dynamic system simulation », *Appl. Mech. Rev.*, vol. 55, n° 6, p. 535–577, 2002.
- [28] J. Ding, G. Bandak, S. B. Leen, E. J. Williams, et P. H. Shipway, « Experimental characterisation and numerical simulation of contact evolution effect on fretting crack nucleation for Ti–6Al–4V », *Tribol. Int.*, vol. 42, n° 11, p. 1651–1662, 2009.